Plasma Sputtered Growth of Ni-Pd Bimetallic Nanoparticles on Carbon Nanotubes for Toluene Sensing

Selene Acosta [1], Juan Casanova-Chafer [2,3], Eduard Llobet [3], Axel Hemberg [4], Mildred Quintana [5,6], and Carla Bittencourt [2,*]

[1] CONACYT-Centro de Investigación en Ciencias de la Salud y Biomedicina, Universidad Autónoma de San Luis Potosí, Av. Sierra Leona 550, Lomas de San Luis, 78210, San Luis Potosí, México

[2] Chimie des Interactions Plasma Surface, Institute for Materials Science and Engineering, Université de Mons, Place du Parc 23, 7000, Mons, Belgium

[3] Departament d'Enginyeria Electronica, Universitat Rovira i Virgili, Països Catalans 26, 43007 Tarragona, Spain

[4] Materia Nova Research Center, 7000 Mons, Belgium; Axel.hemberg@materianova.be

[5] Centro de Investigación en Ciencias de la Salud y Biomedicina, Universidad Autónoma de San Luis Potosí, Av. Sierra Leona 550, Lomas de San Luis, 78210, San Luis Potosí, México

[6] Facultad de Ciencias, Universidad Autónoma de San Luis Potosí, Av. Parque Chapultepec 1570, privadas del Pedregal, 78295, San Luis Potosí, México.
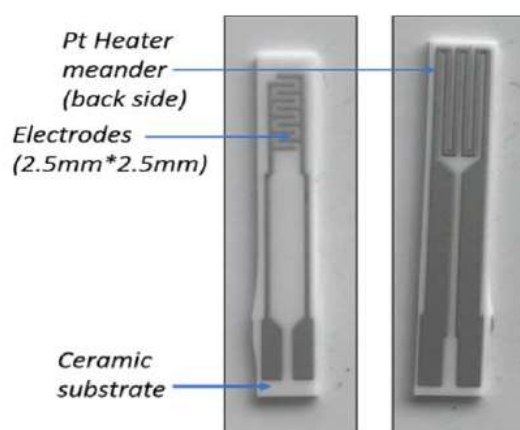*Correspondence: carla.bittencourt@umons.ac.be

Figure S1. Commercially alumina substrates (CeramTech, GmbH) used for gas sensing tests.
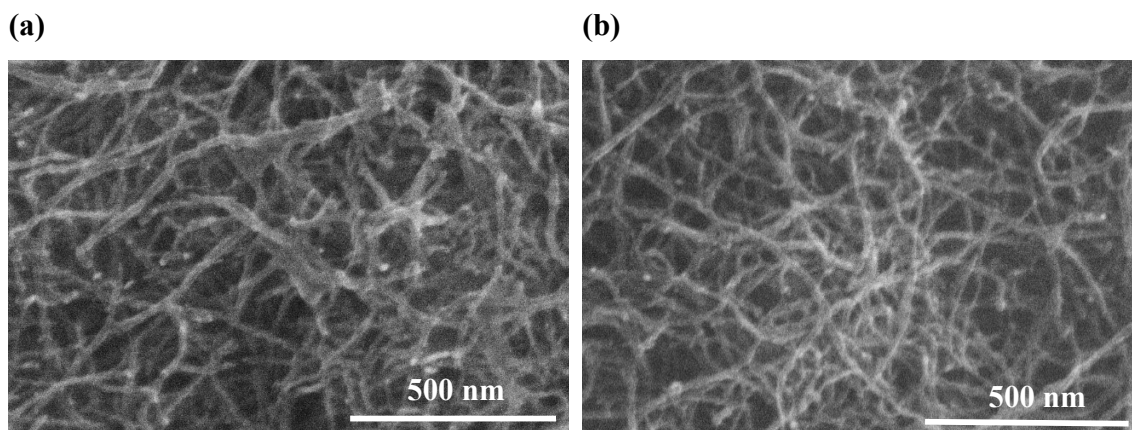
(a) **(b)**

Figure S2. FESEM images of 5-Ni-Pd-OxCNTs (**a**) and 30-Ni-Pd-OxCNTs (**b**). Bright spots reveal the presence of bimetallic nanoparticles.

Table S1. Relative atomic concentration of elements on CNTs samples before and after deposition of Pd and Ni-Pd nanoparticles. Data obtained from XPS analysis.

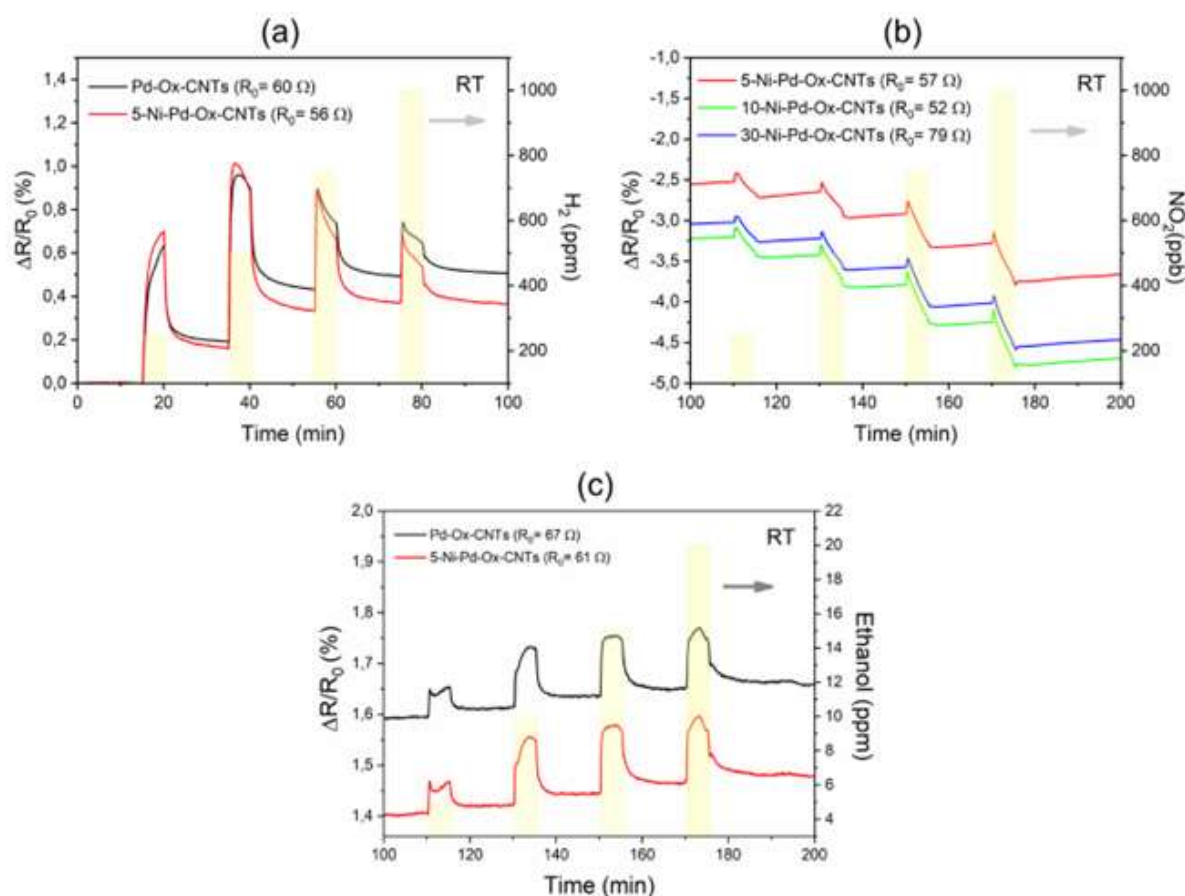| Sample	Relative Atomic Concentration (at. %)			
	Carbon	Oxygen	Palladium	Nickel
Pristine-CNTs	92.1	7.9	-	-
Ox-CNTs	77.9	22.1	-	-
Pd-Ox-CNTs	72.0	25.8	2.2	-
5-Ni-Pd-Ox-CNTs	66.3	30.1	2.8	0.8
10-Ni-Pd-Ox-CNTs	65.4	29.8	2.9	1.9
30-Ni-Pd-Ox-CNTs	65.3	27.6	1.3	5.8

Figure S3. Response and recovery curves of Pd-Ox-CNTs and Ni-Pd-Ox-CNT active layers for a variable concentration of (**a**) H_2; (**b**) NO_2; (**c**) Ethanol. The measurements were carried out at room temperature. The samples not shown in each graph did not respond to that specific gas.

Table S2. Linear equations for the calibration curves for the four sensors tested.

Sample	Linear Fit
Pd-Ox-CNTs	$y = 0.129 + 0.050x$
5-Ni-Pd-Ox-CNTs	$y = 0.116 + 0.044x$
10-Ni-Pd-Ox-CNTs	$y = 0.007 + 0.025x$
30-Ni-Pd-Ox-CNTs	$y = 0.037 + 0.042x$

Table S3. FWHM and position of the components used to reproduce the Ni2p spectra. % relative contribution to the peak intensity.

	Ni^0	Ni^{2+}	Ni^{3+}	Satellite
5-Ni-Pd-Ox-CNTs				
FWHM	1.5	2.0	2.0	5.0
Position	853.3	856.0	857.9	861.4
%	13%	37%	13%	37%
10-Ni-Pd-Ox-CNTs				
FWHM	2.0	2.1	2.2	5.0
Position	853.1	856.1	858.4	862.2
%	3%	40%	13%	44%
30-Ni-Pd-Ox-CNTs				
FWHM	2.2	2.1	2.2	5.0
Position	853.8	856.0	858.2	861.9
%	5%	40%	11%	44%